Electronic Supplementary Information

Self-supporting Nano-porous Carbon Nanosheet with Organized sp^2-C Network for Unprecedented Catalytic Performance in Room-temperature H_2S Oxidization

Feng Hu, [‡a] *Huan Chen,* [‡a] *Zhengliang Zhang,*[a] *Bo Niu,*[a] *Yayun zhang* [*ab] *and Donghui Long* [*ab]

[a] State Key Laboratory of Chemical Engineering, East China University of Science and Technology, Shanghai 200237, China.

[b] Key Laboratory for Specially Functional Materials and Related Technology of the Ministry of Education, School of Chemical Engineering, East China University of Science and Technology, Shanghai 200237, China

[*] Corresponding authors:

E-mail: yy.zhang@ecust.edu.cn (Yayun Zhang);

longdh@mail.ecust.edu.cn (Donghui Long)

[‡] These authors contributed equally to this work

ABSTRACT: Graphene-based carbons have emerged promising applications in non-metal catalysis, but is challenged by interlayer stack and poor porosity. Herein, the concept of graphene-liked carbons is proposed with porous carbon nanosheets (PCNs) being prepared via a melt-foaming strategy. PCNs show abundant pore structure and organized sp^2-C network around nanopores. Moreover, the robust and curved nanosheet keeps spatially isolated and is thus totally stack free. The unimpeded accessibility to functional groups, defects and sp^2-C network enables PCNs with outstanding activity of activating oxygen and high compatibility as carbon support. Thus, alkali-modified PCNs present appalling catalytic oxidation of hydrogen sulfide with unprecedented sulfur capacity up to 10.7g H_2S /g catalyst, 3-fold than that of graphene-based benchmark counterparts. This study provides new insight into the rational design of next-generation carbon catalyst, opening up exciting opportunities for diverse applications.

Table of Contents

1. Supplementary Figures

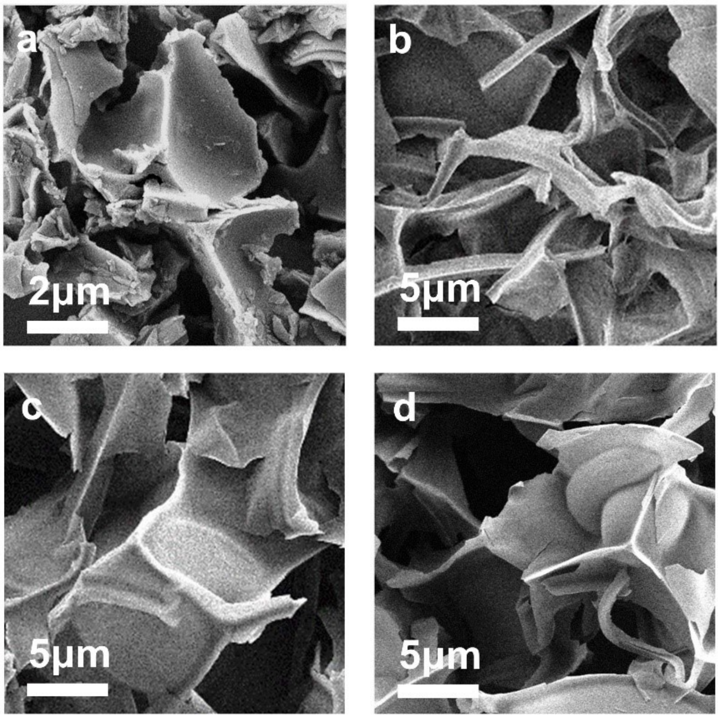

Figure S1. SEM images of (a) PCNs-400, (b) PCNs-500, (c) PCNs-600, (d) PCNs-700.

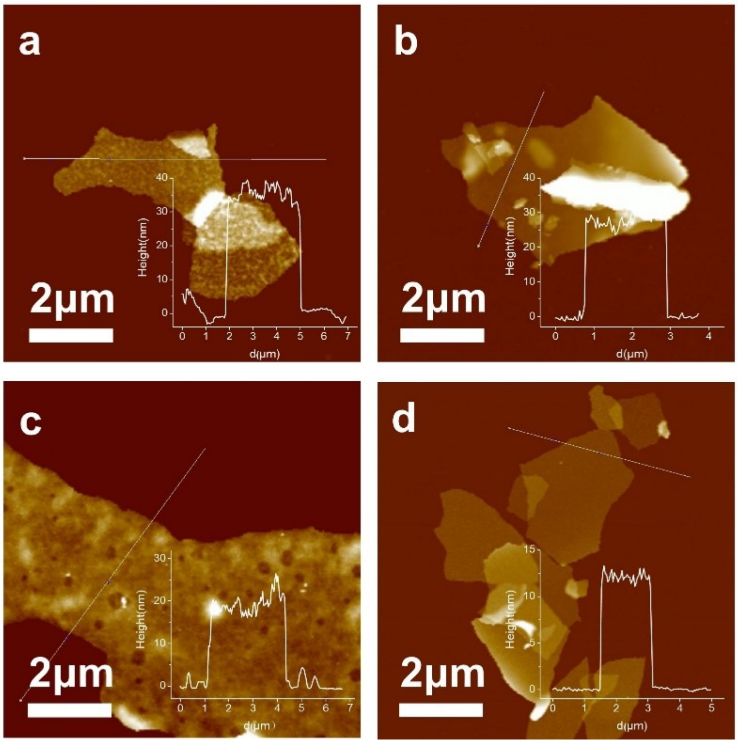

Figure S2. AFM images of (a) PCNs-400, (b) PCNs-500, (c) PCNs-600, (d) PCNs-700.

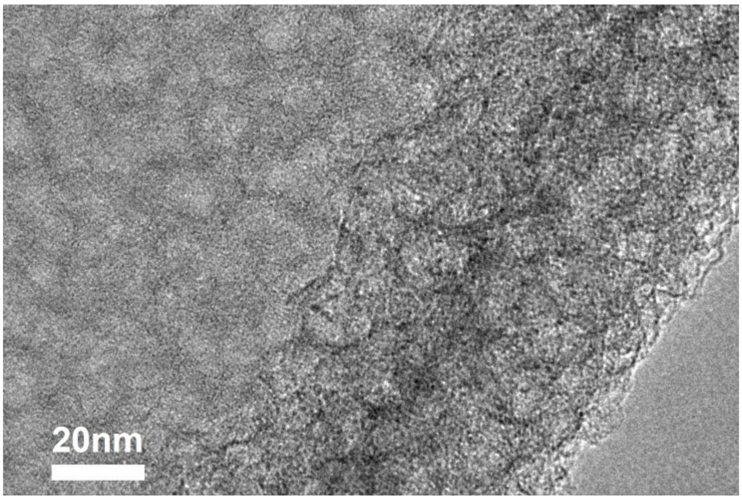

Figure S3. TEM images of PCNs-600.

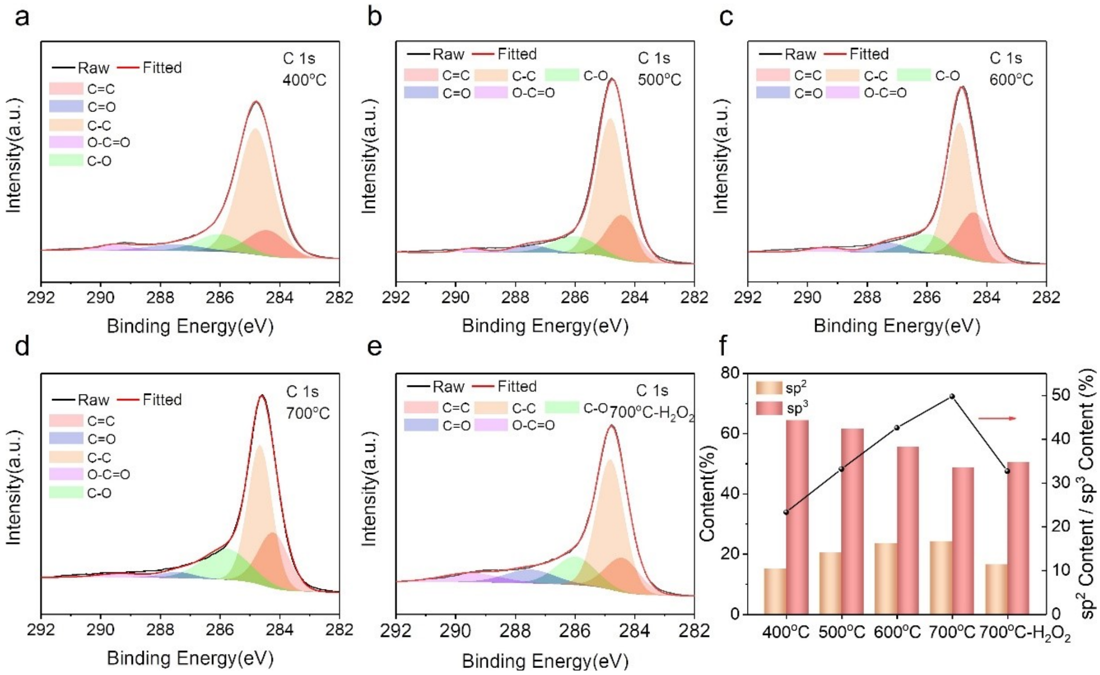

Figure S4. XPS of C1s of (a) PCNs-400, (b) PCNs-500, (c) PCNs-600, (d) PCNs-700, (e) PCNs-700-H_2O_2. (f)sp^2-C, sp^3-C content, and their ratio of PCNs-T.

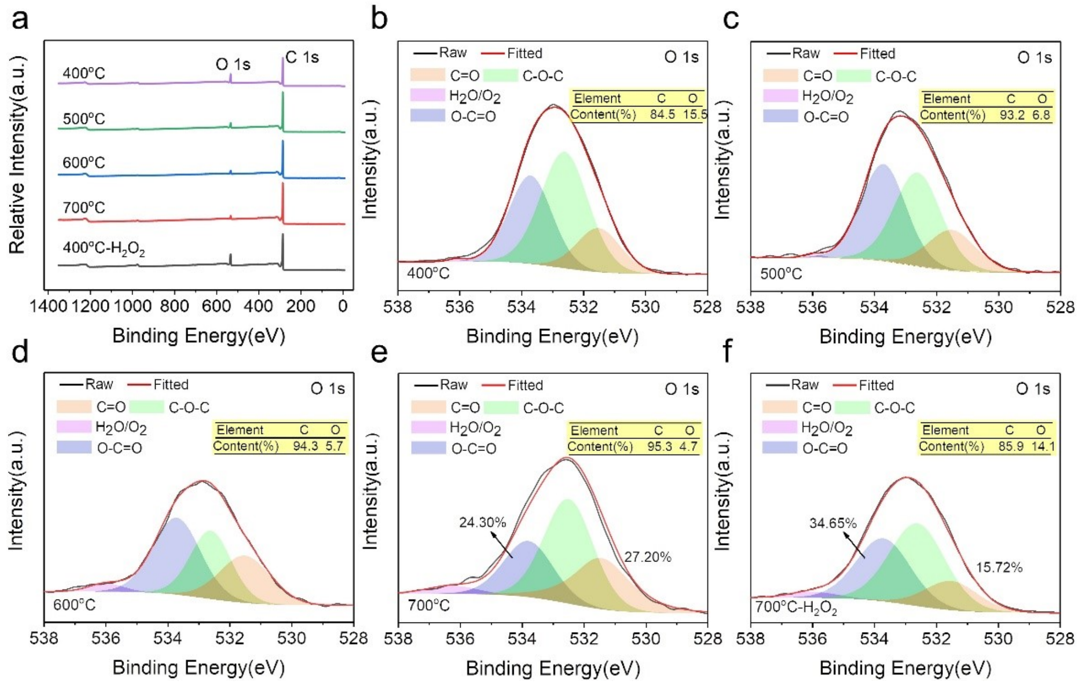

Figure S5. (a) XPS full spectrum of PCNs-T. XPS of O1s of (b) PCNs-400, (c) PCNs-500, (d) PCNs-600, (e) PCNs-700, (f) PCNs-700-H_2O_2.

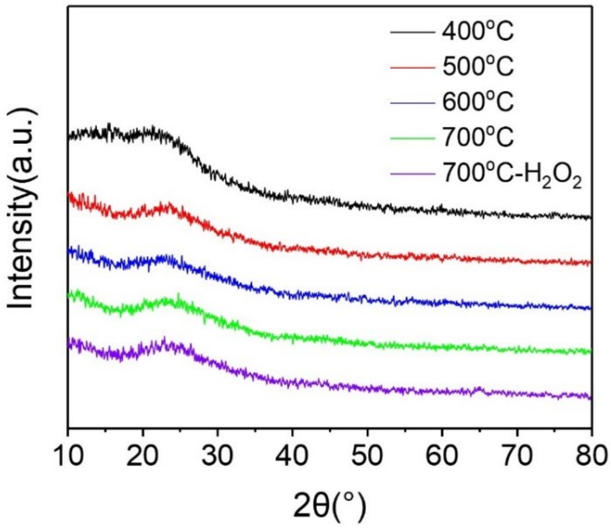

Figure S6. The XRD patterns of PCNs-T.

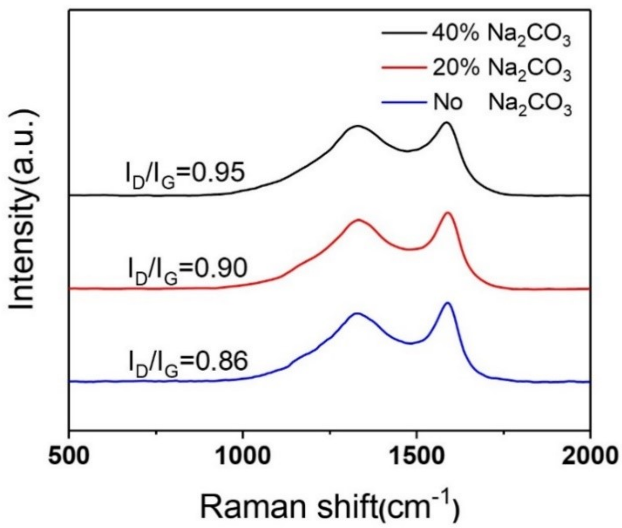

Figure S7. The Raman spectra of PCNs-700-x.

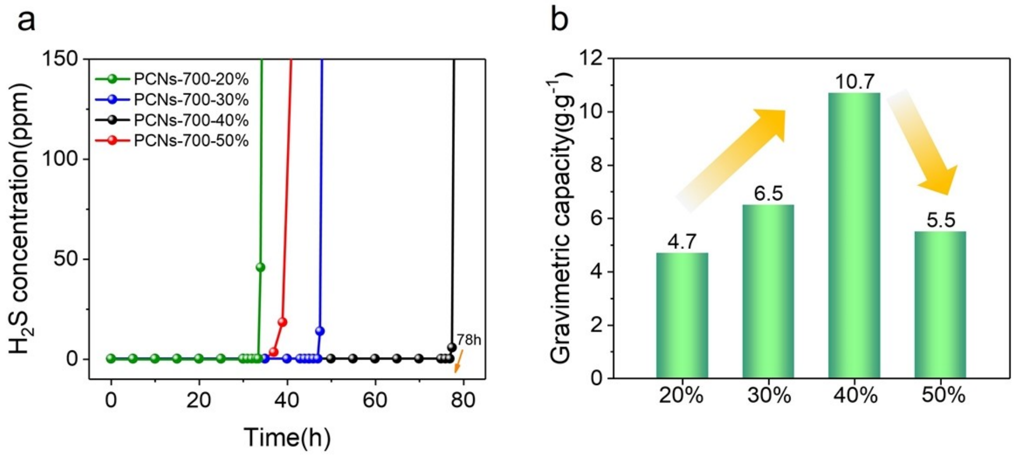

Figure S8. (a) Breakthrough curves and (b) the corresponding breakthrough sulfur capacities of PCNs-700 with different Na_2CO_3 loadings under O_2/H_2S=10:1.

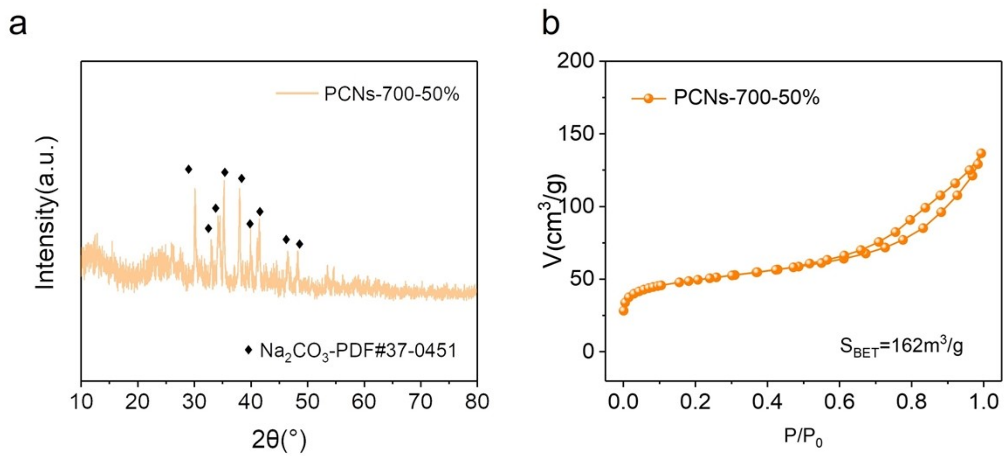

Figure S9. (a) The XRD patterns and (b) N_2 adsorption-desorption isotherms of PCNs-700-50%

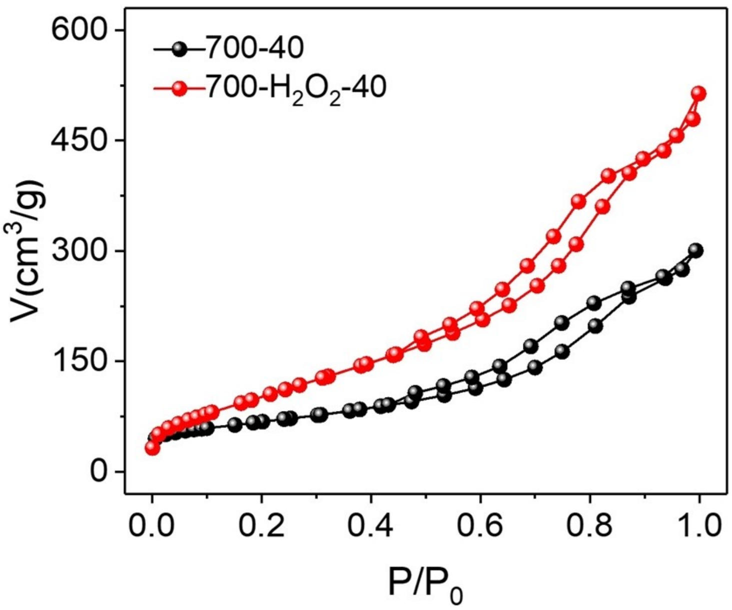

Figure S10. N_2 adsorption-desorption isotherms of PCNs-700-40% and PCNs-700-H_2O_2-40%.

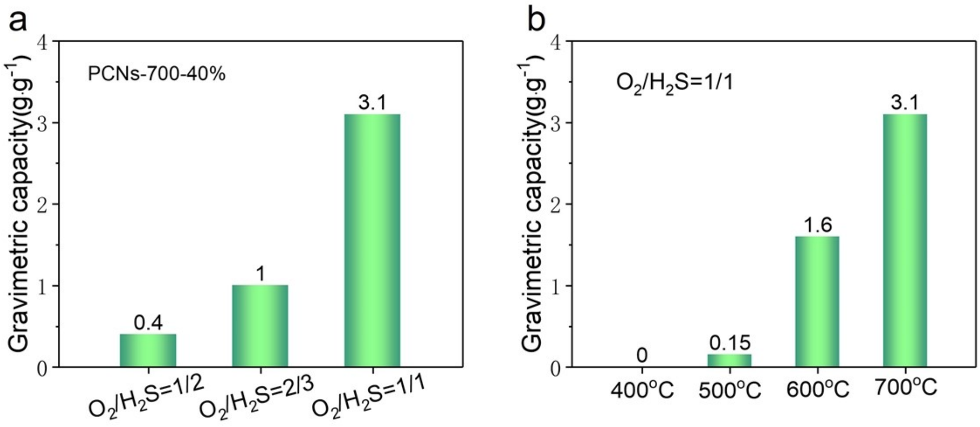

Figure S11. (a) Breakthrough capacity of PCNs-700-40% under different ratio of O_2 to H_2S. (b) Breakthrough capacity of PCNs-T-40% under O_2/H_2S=1:1.

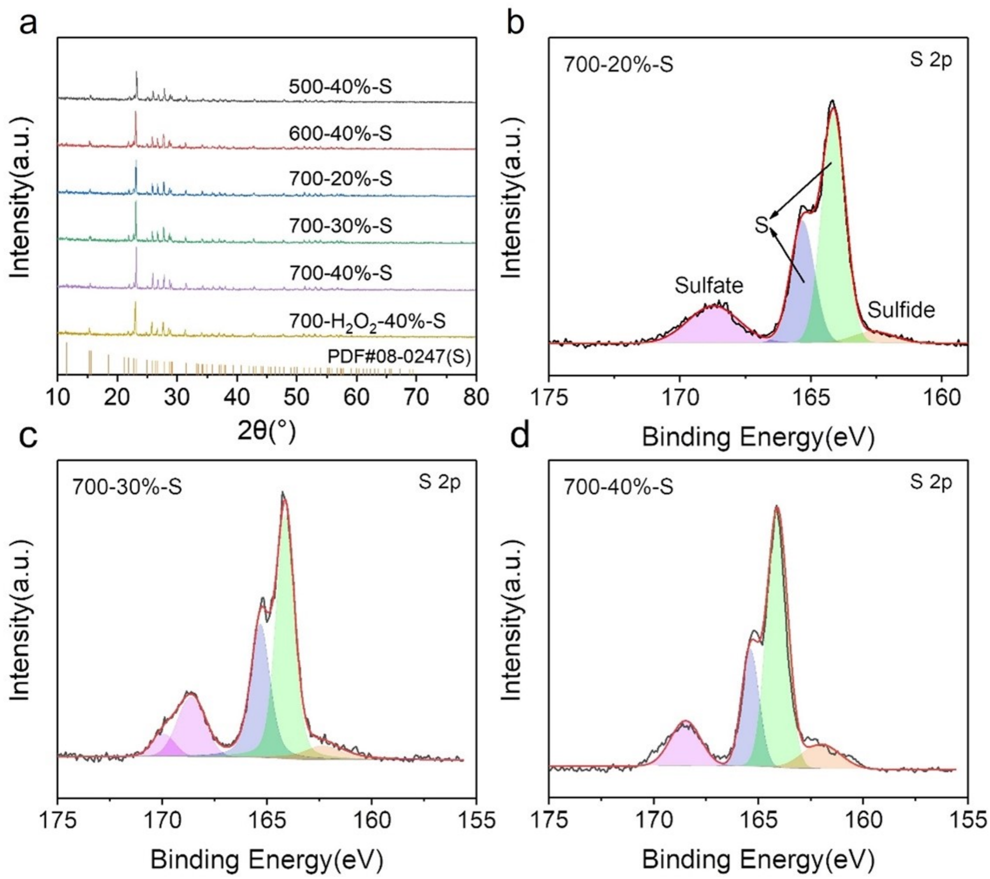

Figure S12. (a) The XRD patterns of PCNs-T-x-S. XPS of S 2p of (b)PCNs-700-20%-S, (C) PCNs-700-30%-S, (d) PCNs-700-40%-S.

2. Supplementary Tables

Table S1. Surface area and porosity properties of all PCNs-T.

Sample	S_{BET}[a] (m^2/g)	V_t[b] (cm^3/g)	S_{mic}[c] (m^2/g)	V_{mic}[d] (cm^3/g)
PCNs-400	48	0.16	-	-
PCNs-500	406	0.5	42	0.02
PCNs-600	536	0.68	226	0.12
PCNs-700	768	1.36	107	0.05
PCNs-700 -H_2O_2	585	1.05	40	0.02

[a] Specific surface area calculated by using multipoint BET theory.

[b] Total pore volume calculated from nitrogen physisorption isotherm at p/p_0=0.99.

[c,d] Micropore specific surface area and pore volume calculated by using t-plot method.

Table S2. Relative contents of different oxygen-containing groups in O1s spectra.

	C=O	**C-O-C**	**O-C=O**	**H_2O/O_2**
PCNs-400℃	17.20%	48.85%	33.54%	0.41%
PCNs-500℃	18.01%	40.93%	40.42%	0.64%
PCNs-600℃	26.27%	30.52%	40.00%	3.21%
PCNs-700℃	27.20%	25.15%	44.30%	3.35%
PCNs-700-H_2O_2	15.72%	46.59%	34.65%	3.03%

Table S3. Surface area and porosity properties of all PCNs-T-40%.

Sample	**S_{BET}(m²/g)**	**V_t (cm³/g)**	**S_{mic}(m²/g)**	**V_{mic} (cm³/g)**
PCNs-400-40%	27	0.12	-	-
PCNs-500-40%	105	0.16	-	-
PCNs-600-40%	302	0.37	11	0.01
PCNs-700-40%	238	0.46	40	0.02
PCNs-700-H_2O_2-40%	246	0.49	30	0.01

Table S4. Recently reported carbon-based catalysts for H_2S oxidation.

No.	Catalyst	$^{a}C_{H2S}$ (ppm)	^{b}t(°C)	$^{c}O_2$(%)	^{d}WHSV(g $g^{-1}h^{-1}$)	$^{e}Q_B$(g g^{-1})	Ref
1	Na_2CO_3/PCNs	2500	25	1	45	10.7	This work
2	Alkaline graphene aerogels	1000	30	1	75	3.19	4
3	Na_2CO_3/Nitrogen-doped mesoporous carbon nanosheets	1000	RT	2	375	1.37	6
4	Alkaline carbon nanotubes	1000	30	1	112.5	1.51	7
5	Alkaline mesoporous carbon spheres	1000	30	1	/	2.46	8
6	Alkaline mesoporous carbon	1000	25	1	75	2.65	9
7	Na_2CO_3/carbon aerogels	1000	30	1	/	1.61	10
8	$CuFe_2O_4$/AC	10000	RT	21	/	0.67	11
9	MgO/rGO	1000	30	1	75	3.11	12
10	IAC	600	30	0.12	6	0.42	13
11	Nitrogen-rich mesoporous carbons	1000	30	/	37.5	2.77	14

$^{a}H_2S$ concentration in the inlet gas. ^{b}Reaction temperature. $^{c}O_2$ concentration in the inlet gas. ^{d}Weight hourly space velocity, calculated by $WHSV = \frac{F \cdot \rho_{gas}}{m_{cat.}}$, where F is the flow rate (L/h), ρ_{gas} is the density of inlet gas (g/L), and $m_{cat.}$ is the weight of used catalyst (g). ^{e}Breakthrough sulfur capacity, g H_2S/g cat.

Reference:

1 Y. Pan, M. Chen, Z. Su, K. Wu, Y. Zhang and D. Long, Two-dimensional CaO/carbon heterostructures with unprecedented catalytic performance in room-temperature H_2S oxidization, *Applied Catalysis B: Environmental,* 2021, **280**, 119444.

2 Y. Zou, W. Li, L. Yang, F. Xiao, G. An, Y. Wang and D. Wang, Activation of peroxymonosulfate by sp^2-hybridized microalgae-derived carbon for ciprofloxacin degradation: Importance of pyrolysis temperature, *Chemical Engineering Journal,* 2019, **370**, 1286-1297.

3 Y. Li, Y. Lin, Z. Xu, B. Wang and T. Zhu, Oxidation mechanisms of H_2S by oxygen and oxygen-containing functional groups on activated carbon, *Fuel Processing Technology,* 2019, **189**, 110-119.

4 Y. Pan, M. Chen, M. Hu, M. Tian, Y. Zhang and D. Long, Probing the room-temperature oxidative desulfurization activity of three-dimensional alkaline graphene aerogel, *Applied Catalysis B: Environmental*, 2020, **262**, 118266.

5 Y. Yuan, L. Huang, T. C. Zhang, L. Ouyang and S.Yuan, One-step synthesis of $ZnFe_2O_4$-loaded biochar derived from leftover rice for high-performance H_2S removal, *Separation and Purification Technology*, 2021, **279**.

6 Z. Yu, X. Wang, Y. Hou, X. Pan, Z. Zhao, and J. Qiu, Nitrogen-doped mesoporous carbon nanosheets derived from metal-organic frameworks in a molten salt medium for efficient desulfurization, *Carbon*, 2017, **117**, 376-382.

7 Q. Chen, J. Wang, X. Liu, X. Zhao, W. Qiao, D. Long, and L. Ling, Alkaline carbon nanotubes as effective catalysts for H_2S oxidation, *Carbon*, 2011, **49**, 3773-3780.

8 Z. Zhang, J. Wang, W. Li, M. Wang, W. Qiao, D. Long, and L. Ling, Millimeter-sized mesoporous carbon spheres for highly efficient catalytic oxidation of hydrogen sulfide at room temperature, *Carbon*, 2016, **96**, 608-615.

9 Z. Zhang, W. Jiang, D. Long, J. Wang, W. Qiao, and L. Ling, A General Silica-Templating Synthesis of Alkaline Mesoporous Carbon Catalysts for Highly Efficient H_2S Oxidation at Room Temperature, *ACS Applied Materials & Interfaces*, 2017, **9**, 2477-2484.

10 Q. Chen, J. Wang, X. Liu, Z. Li, W. Qiao, D. Long, and L. Ling, Structure-dependent catalytic oxidation of H_2S over Na_2CO_3 impregnated carbon aerogels, *Microporous and Mesoporous Materials*, 2011, **142**, 641-648.

11 S. Chen, Y. Guo, J. Zhang, Y. Guo, and X. Liang, $CuFe_2O_4$/activated carbon adsorbents enhance H_2S adsorption and catalytic oxidation from humidified air at room temperature, *Chemical Engineering Journal*, 2022, **431**, 134097.

12 H. Xu, Y. Pan, F. Hu, B. Niu, Y. Zhang, and D. Long, Anti-corrosion MgO nanoparticle-equipped graphene oxide nanosheet for efficient room-temperature H_2S removal, *Journal of Materials Chemistry A*, 2022, **10**, 18308-18321.

13 Y. Xiao, S. Wang, D. Wu, and Quan Yuan, Catalytic oxidation of hydrogen sulfide over unmodified and impregnated activated carbon, *Separation and Purification Technology*, 2008, **59**, 326-332.

14 F. Sun, J. Liu, H. Chen, Z. Zhang, W, Qiao, D Long, and L. Ling, Nitrogen-Rich Mesoporous Carbons: Highly Efficient, Regenerable Metal-Free Catalysts for Low-Temperature Oxidation of H_2S, *ACS Catalysis*, 2013, **3**, 862−870.